Case Studies in Thermal Engineering 22 (2020) 100776

Contents lists available at ScienceDirect

Case Studies in Thermal Engineering

journal homepage: http://www.elsevier.com/locate/csite

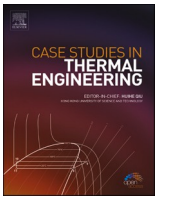

Heat transfer measurements of Polyalpha-Olefin- boron nitride nanofluids for thermal management and lubrication applications

Ahmad K. Sleiti

Department of Mechanical & Industrial Engineering, College of Engineering, Qatar University, Qatar

ARTICLE INFO

Keywords:
Nanofluids
Thermophysical properties
Heat transfer enhancement
Polyalpha-olefin
Boron nitride

ABSTRACT

In this paper, the first study is reported combining Polyalpha-Olefin (PAO) oil with hexagonal Boron Nitride (hBN) to produce new class of nanofluids for heat transfer and lubrication applications. The heat transfer performance of the nanofluids is studied experimentally along with their viscosity, specific heat, thermal diffusivity and thermal conductivity. Thermophysical properties relations are derived as a function of temperature and nano particle concentration. Heat transfer experiments are conducted for both the PAO base fluid and nanofluid as a function of Reynolds number. It is found that PAO/hBN nanofluids exhibit Newtonian behavior as a function of temperature (from −20 to 70 °C) and volume concentration (0.25–1%). The viscosity decreases with temperature for both base fluid and PAO/hNB nanofluids and increases with concentration. The specific heat increases with temperature by 44% from 45 °C to 95 °C for pure PAO and by 48% for nanofluid with 1% concentration. The thermal conductivity of nanofluids is significantly higher than that of pure PAO and it increases by increasing hBN concentration. The thermal conductivity decreases with temperature for pure PAO and nanofluids unlike other nanofluids. The heat transfer enhancement in terms of Nussel Number showed average and maximum values of 10%–13%, 17%–20% and 26%–29% for hBN concentration of 0.25%, 0.6% and 1%, respectively. Two competing phenomena affect the heat transfer performance: the increase/decrease in resistance to thermal diffusion sublayer when thermal conductivity increases and viscosity decreases, respectively. For the PAO/hBN nanofluids, the increase in thermal conductivity caused the heat transfer enhancement.

1. Introduction

The quest by various technologies for boosting the convective cooling performance to dissipate heat has never been so intensive, especially for thermal management applications of solar energy systems, electric machines and electronics, and manufacturing processes. Therefore, new cooling technologies need to be developed with superior thermal performance, without penalties (such as increasing the size and volume of the system), and without increasing the pumping requirements. Nanofluids for heat transfer applications have great potential to meet this ever-growing cooling demand. Nanofluids are prepared by dispersing nanoparticles (10–100 nm particle size) in water or oil base fluids that can be used, in addition to heating and cooling [1], in other diverse applications [2–7]. Although an overwhelming number of publications is available in open literature on experimental and theoretical work of nanofluids, however, nanofluids with Boron Nitride (BN) nanoparticles and Polyalpha-Olefin (PAO) oil as base fluid for cooling applications have not been reported. BN has favorable thermophysical properties and BN nanofluids with water base fluid showed

E-mail address: asleiti@qu.edu.qa.

https://doi.org/10.1016/j.csite.2020.100776
Received 25 July 2020; Received in revised form 27 October 2020; Accepted 29 October 2020
Available online 2 November 2020

Nomenclature

Symbol Description Units

A, B, C	Curve fit parameters
Cp	Specific heat J/kg.K
D	Diameter m
h	Convection heat transfer coefficient W/m^2.K
k	Thermal conductivity W/m.K
L	Length of test section m
Mo	Mouromtseff number
$\dot{m}$	Mass flow rate kg/s
*N*u	Nusselt Number
p	Pressure Pa
P	Perimeter m
Pr	Prandtl number
q	Heat transfer rate W
Re	Reynolds Number
T	Temperature ^{o}C or K
U	Velocity m/s
x	Location in x direction m

Greek symbols

α	Thermal diffusivity m^2/s
f	Frictional coefficient
φ	Volumetric concentration %
μ	Viscosity Pa.s
ρ	Density kg/m^3

Subscripts

c1, c2 …. c7	Thermocouple number
conv	Convection
D	Diameter
in	inlet
m	mean
out	outlet
s	surface

Abbreviations

BN	Boron Nitride
PAO	Polyalpha-Olefin

enhanced heat transfer performance and thermophysical properties for cooling applications [8]. PAO is used in varies industries as lubricant and as a cooling fluid [9,10]. Combining PAO with NB to produce nanofluids for improved cooling and lubrication performances seems very attractive idea and is the main objective of the present study. The thermophysical properties and heat transfer characteristics of different nanofluids are discussed briefly in the next subsections, emphasizing the use of PAO and BN.

Several studies in open literature investigated the thermal conductivity (k) of nanofluids [11], almost all of which reported significant enhancement in k over the base fluids. An increase in k of 60–70% was reported by Hong et al. [12] using single-wall CNT nanoparticle in PAO base fluid. The enhancement found by Yu et al. [13] was 50–60% of water with silicon carbide nanoparticles of volumetric concentration 3.7%. Singh et al. [14] have shown 28% enhancement in k of SiC/water nanofluid. Liu et al. [15] reported 30% enhancement for CNT–synthetic/engine oil nanofluids. For Multi Walled Nano Tubes and α-Olefin oil nano fluid, Choi et al. [16] found 150% enhancement in k. The thermal conductivity of nanofluids with PAO as base fluid, were tested with aluminum oxide and MWCNT nanoprticles in Refs. [17]. They found that nanoparticle concentration enhanced k more than the Hamilton and Crosser's model predicted due to clustering and thus, they developed a modified model that accounts for that. The thermophysical properties of hexagonal boron nitride (hBN) nanofluids with DI water, ethylene glycol (EG) and EG–DI water mixture base fluids were investigated by Ilhan et al. [18] with particle volume concentration from 0.03% to 3%. They found that the hBN nanofluids k is much higher than the base fluids with water based hBN nanofluids showing significant increase in k compared to the viscosity increase. In addition to the experimental studies above, the thermal conductivity of nanofluids can be studied using artificial neural network and intelligence methods as reported in Ref. [19–21].

Several heat transfer studies of nanofluids for thermal management can be found in Ref. [22–27] using different types of nanoparticles and base fluids. A recent study of friction factor and heat transfer coefficient for SiO_2 –ethylene glycol/water (50 wt%)

nanofluids [28], found 25% enhancement in the heat transfer coefficient of the nanolfuid. However, the challenge in cooling applications is still persisting, when oil is used as base fluid, to enhance the thermal conductivity side by side with reasonable increase of viscosity [29]. To address this challenge, researchers in Ref. [29] used several oils and fuels including transformer oil, mineral oil, silicon oil, hydrocarbon fuels, biodiesel, and organic solutions as the base fluids for heat transfer augmentations. They highlighted worthy enhancements in heat transfer performance. Applications of nanofluids as heat transfer fluids in solar energy systems have drawn the attention of researchers and engineers. Refiei et al. [30] used nanofluids of MWCNT/oil to investigate a solar organic Rankine cycle performance. Moh et al. [31] reported a cooling application using Graphene nanofluids on flat solar panel. Abro et al. [32] performed an interesting heat transfer study using rotating Jeffrey nanofluids to enhance the performance of solar energy systems.

The use of oil base nanofluids in electric machines for both electric insulation and heat dissipation has drawn the attention of researchers and engineers for the last three decades. Nanofluids with insulating oil base fluids were found in Ref. [33] to be stable and homogeneous with advanced performance of both cooling and electric insulation. In addition to insulation and cooling applications, a variety of nanoparticles can be used as lubricant additives (reviewed by Gulzar et al. [34]) with potentially favorable friction and wear properties.

While many publications have studied viscosity of different oil base nanofluids, only few investigated PAO nanofluids and its heat transfer performance. Moreover, as mentioned before, the potential of using BN as nanoparticles in PAO oil base nanofluids was not explored before. Lubrication properties of PAO are attractive and there is potential to improve these properties by adding nanoparticles to the base oil (PAO). There are many proofs in open literature confirming that adding nano particles to lubricants improves their lubrication properties. For example, Wang et al. [35] reported that Al2O3 nanofluids with base vegetable oil could reduce the sliding friction remarkably by forming a reduced friction film on the tested surface. A 19.3% reduction in the average friction coefficient was achieved with 65% increase in mass wearing ratio compared with palm oil. Another evidence was reported by Ramón-Raygoza et al. [36] who manufactured lubricant nanofluids with multi-layer graphene (MLG), (MLG-Cu), and MLG impregnated with polyaniline (MLGPANI) for automotive engines application. They acheived significant reductions in coefficient of friction and wear of 43% and 63%, respectively.

Some studies on using BN with lubricant oils as base fluid have been reported in literature. Wan et al. [37] studied the tribological properties of BN nanolubricant. They recommended an optimal concentration of nanoparticles of 0.1 wt%. Indicating that nanolubricants with small amount of BN exhibit superior tribological performance. Guimarey et al. [38] studied the effects of concentration and morphology of nanoadditives on the thermophysical properties of nanolubricants (NLs) as a function of temperature. They used polyalphaolefin (PAO6) oil with Zirconium oxide (ZrO2) and BN nanoparticles (NPs) and graphene nanoplatelets (GnP) with mole fraction of 0.05 wt% to 2 wt%. They developed correlations for prediction of pressure-viscosity coefficients as a function of concentration and temperature. Other researchers studied different lubricant additives with varying results. For example, Kiu et al. [39] studied the tribological behaviours of graphene nanoparticles as lubricant additive in vegetable oil and recommended optimum concentrations for the best friction performance.

Determination of the viscosity of nanofluids accurately, is very important and is one of the targeted outcomes of the present study. There are several correlations in open literature that predict the viscosity of nanofluids as a function of temperature and nanoparticle concentration [40–45]. These and other correlations available in open literature are usually derived for class of nanofluids and temperature and concentration ranges suitable for their intended applications. However, upon comparison with results obtained in the present study, it was found that these correlations have deviations, in some cases, exceeding ±45% from the measured viscosities. Therefore, a new viscosity correlation is developed in the current study for temperature range from −20 °C up to 70 °C. Many current and future technologies need rapid cooling solutions and better lubrication fluids with reduced friction. To address this, PAO/hNB nanofluids are developed and their rheological characteristics, thermophysical properties and heat transfer performance are investigated experimentally with BN φ of 0.25%, 0.6% and 1% over practical temperature range.

2. Heat transfer measurements

Heat transfer measurements of PAO based nanofluids were reported in open literature for different nano-particle fillers with clear evidence of heat transfer improvement. Nelson et al. [46] conducted fin strip heat transfer experiments using exfoliated graphite nanoparticle fibers in PAO at 0.3 and 0.6 mass concentrations. They observed 10% enhancement, which they partially attributed to the deposited nanoparticals on the surface that enhanced the heat transfer. Heat transfer study of non-Newtonian nanofluids Fe2O3, Al2O3 and CuO nanoparticles in aqueous carboxymethyl cellulose (CMC) base fluid was reported by Naink and Vinod [47] in a shell and helical coil heat exchanger. They used the nanofluid on shell side and water in tube side and they determined the overall heat transfer coefficient and shell-side Nusselt number (*Nu*). They reported significant increase in the rate of heat transfer at higher nanofluid concentrations, shell-side temperatures, stirrer speeds and Dean numbers. Shahmohamadi et al. [48] theoretically and experimentally investigated the tribological performance of carbon nanoparticles in PAO6 oil. Results showed improved heat transfer even at low concentration with higher lubricant viscosity, load carrying capacity and reduced friction. Based on that, the potential of PAO/hBN as an enhanced heat transfer fluid is clear. In this section, details are given for the experimental setup that is designed for testing of the heat transfer characteristics of the developed in this study PAO/hBN nanofluids.

2.1. Heat transfer test setup

The heat transfer test set up is shown by Fig. 1 (a) and (b). The test setup consists of two loops; (1) a transparent plastic piping loop with a Flojet pump FDP 1000 to monitor the pressure and to visualize the flow and (2) the heat transfer closed loop with the nanofluid

maintained at a uniform inlet temperature by circulating the fluid through a BPX Brazed Plate Heat Exchanger model BP400, and the exit temperature from the heat exchanger is controlled by means of a preheater.

The test section is equipped with inlet valve to control the flow rate and an Omega pressure sensor model PX2300, which monitors the test loop for any changes in pressure. The clear plastic pipe allows visualization of the fluid to ensure that the nanofluid is

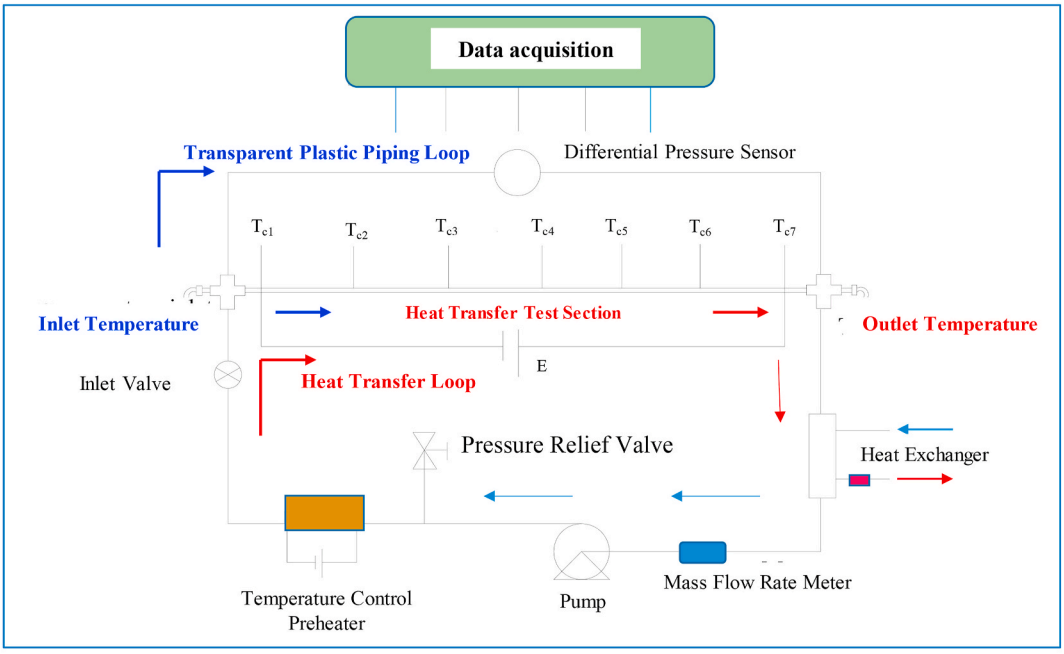

(a)

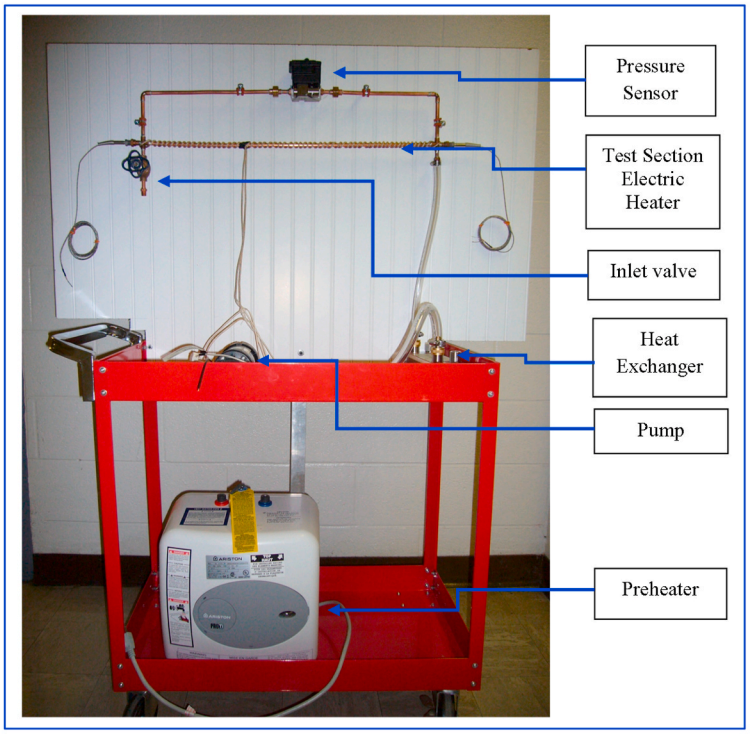

(b)

Fig. 1. Heat transfer test setup – (a) schematic, (b) photo.

thoroughly mixed and air bubbles are not present during testing. The heat transfer test section is made from standard copper tubing having the dimensions 0.700 m × 0.00635 m x 0.120 m. The test loop was instrumented with 7 evenly placed thermocouples to measure the local temperatures (T_{c1} to T_{c7} in Fig. 1) across the test loop, in addition to the 2 temperature sensors attached to each end of the loop to measure the fluid inlet and exit temperatures, respectively. Description of the instruments shown in Fig. 1(a) and (b) are summarized next.

Data acquisition hardware. The Instrument model 100 hardware manufactured by Omega Engineering is compatible with the data that has to be collected. It plugs into a computer via a PCI cable and has a total of 16 digital I/O connections for temperature, pressure and flow inputs. It has an auto-calibration function without the need for digitization.

Temperature measurements. The test setup is instrumented with 11 thermocouple (Tc) to measure temperatures at different locations. Two of them measure the inlet and outlet temperatures of the test section, another two measure the heat exchanger inlet and outlet temperatures and the remaining 7 thermocouples were JT type with probe penetration thermocouple wires manufactured by Omega engineering and spread across the test section. Before the experimental tests, all thermocouples were calibrated they showed an accuracy of 0.2 K.

Flowmeter. The flow meter required for the nanofluid must be able to account for the higher viscosity of the nanofluid. After careful considerations, an oval gear flow meter is used; model FPD10038 from Omega engineering with a range of 3–25 L/min (LPM) flow rate, an accuracy of ±0.5% of reading and repeatability of ±0.03%.

Pump. The flojet pump FPD1000 has a polypropylene construction with heavy duty nylon housings. The pump has a flow rate up to 20 LPM and a maximum operating pressure of 65.5 kPa. It is a self-priming pump that has a built-in pressure switch, which automatically starts and stops the pump instantaneously when the discharge valve is opened and closed. It can run dry without damage and handles liquids up to 71 °C. More than one pump was used when the flow rate needed to be increased.

Heat Exchangers. The heat exchanger subsystem used in this study is the BPX model BP400-020 manufactured by Bell and Gossett. The corrugated plates are made of stainless steel plates that can withstand temperature and pressure up to 150 °C and 3000 kPa, respectively. The heat exchanger also boasts a capacity up to 3000 LPM.

Preheater. A preheater was used to maintain the inlet temperature of the nanofluid. For this purpose, we used an Ariston Pro Ti, which had a heating capacity of 1500 W at an operating pressure of 1000 kPa with a tank volume of 11 L.

2.2. Heat transfer calculations procedure

Determination of the mean temperature T_m at the inlet and exit of the test section is required for the current internal flow and heat transfer analysis. The procedure to find T_m starts with an energy balance for a differential control volume [49], within the heat transfer test section shown in Figs. 1 and 2. The rate of the convection heat of this differential control volume is given as:

$$dq_{conv} = \dot{m}\, C_P\, [(T_m + dT_m) - T_m] = \dot{m}\, C_P dT_m \tag{1}$$

where $\dot{m}$ is the mass flow rate, Cp is the specific heat, T_m and $(T_m + dT_m)$ is the fluid mean temperature at the inlet and outlet of the differential control volume, respectively.

Integrating from the inlet to outlet of the test section,

$$q_{conv} = \dot{m} C_P \left(T_{m,out} - T_{m,in}\right) \tag{2}$$

where $T_{m,out}$ and $T_{m,in}$ are the mean temperatures at the outlet and inlet of the test section, respectively.

Also dq_{conv} can be defined as the product of the heat flux and the differential surface area:

$$dq_{conv} = q_s^{''}\, (P\, dx) = h\, (T_s - T_m)\, P\, dx \tag{3}$$

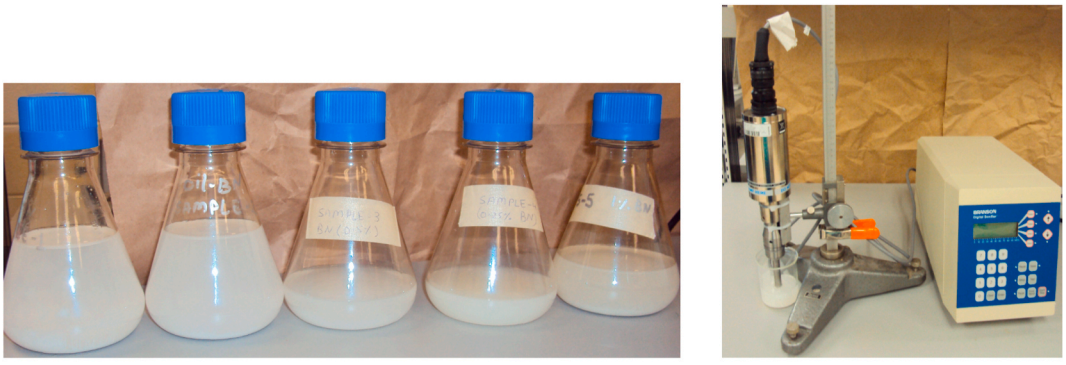

(a) (b)

Fig. 2. (a) Samples prepared with different loadings of BN from 0.25% to 3%. (b) Ultrasound sonicate for 6–7 h.

where P is the perimeter of the pipe, h is the convective heat transfer coefficient and T_s is the surface temperature of the pipe of the test section measured by thermocouples.

Substituting Eq (3) into Eq (1) and rearranging, the differential equation from which T_m may be determined is:

$$\frac{dT_m}{dx} = \frac{q_s'' P}{\dot{m} C_P} = \frac{P}{\dot{m} C_P} h (T_s - T_m) \tag{4}$$

For Uniform Surface Heat Flux (USHF) as in the current study, this equation becomes

$$\frac{dT_m}{dx} = \frac{q_s'' P}{\dot{m} C_P} \tag{5}$$

which is not a function of the longitudinal direction x. Now T_m as a function of x can be calculated as:

$$T_m\left(x\right) = \frac{q_s'' P}{\dot{m} C_P} x \tag{6}$$

The total heat rate is:

$$q_{conv} = q_s'' P L = h (T_s - T_m) P L \tag{7}$$

where L is the length of the heat transfer test section.

The convective heat transfer coefficient, h is calculated from Eq. (7) and then used to calculate Nusselt number:

$$Nu = \frac{h D}{k} \tag{8}$$

where D is the pipe diameter and k is the thermal conductivity of the fluid.

The above Equations are used to calculate the heat transfer performance of the pure PAO and the nanofluids, where the mass flow rate, fluid temperatures, surface temperatures and the thermophysical properties of the nanofluids are obtained from measurements as detailed in the sections below.

For calibration and comparison purposes, the measured Nu of the pure PAO is compared to correlations available in Ref. [49]. Two correlations are used; Sieder and Tate correlation [49] and Gnielinski [50]. Sieder and Tate correlation given in Eq. (9) is used for its accurate results for flows characterized by large property variations as in the current study.

$$Nu_D = 0.027 Re_D^{4/5} Pr^{1/3} \left(\frac{\mu}{\mu_s}\right)^{0.14} \tag{9}$$

This correlation is valid for $Re_D \geq 10{,}000$, $L/D \geq 10$ and $0.7 \leq Pr \leq 16{,}7000$, where Pr is the Prandtl number, μ is the fluid viscosity evaluated at T_m and μ_s is the fluid viscosity evaluated at T_s. Re_D is the Reynolds number with the pipe diameter D as the characteristic length:

$$Re_D = \frac{\rho U D}{\mu} \tag{10}$$

where U is the fluid average velocity calculated from the measured mass flow rate.

Using Eq. (9) could result in large errors [49]. Another correlation, valid over a large Re range is provided by Gnielinski [50]:

$$Nu_D = \frac{(f/8)(Re_D - 1000) Pr}{1 + 12.7 (f/8)^{1/2} (Pr^{2/3} - 1)} \tag{11}$$

The correlation is valid for $0.5 \leq Pr \leq 2000$ and $3000 \leq Re_D \leq 5 \times 10^6$. The friction factor f may be obtained from

$$f = (0.790 \ln Re_D - 1.64)^{-2} \quad 3000 \leq Re_D \leq 5 \text{ x } 10^6 \tag{12}$$

In using Eq. (11), fluid properties are evaluated at Tm.

3. Results and discussion

3.1. PAO/hBN nanofluids preparation

The PAO nanofluid is prepared by dispersion of BN powder in PAO oil. The BN used is 99.5% pure hexagonal Boron Nitride (hBN) powder from M K Impex Canada with average particles of 70 nm and the its density is 2.26 gm/cm^3. The PAO is DURASYN_ 166; a commercial Polyalpha-olefin oil product purchased from Chemcentral (Chicago, IL, USA). Nanofluid samples with BN φ of 0.25%, 0.6% and 1% were prepared. For preparing the 1% by volume sample, oleic acid surfactant was used. The samples then were placed on a magnetic stirrer for more than 30 min and then in ultrasonic agitator (Branson Digital Sonifier, model 450) for 350 min for the 0.25%

and 0.6% samples and 430 min for the 1% sample to ensure uniform dispersion of the nanoparticles, see Fig. 2.

3.2. Measurements and analysis of the rheological properties of PAO/hBN nanofluids

The viscosity of the PAO/hNB nanofluids is measured and used in calculating Re of the flow. The experimental setup for measuring the rheological property of PAO/hBN nanofluids is an AR-G2 rheometer (TA Instruments), a combined motor and transducer (CMT) instrument. The test fluid sample size is approximately 1.5 ml and the temperature of the test fluid is controlled between −20 °C and 70 °C by a water circulator chamber. Different data were taken including rotational speed of the spindle (RPM), torque, viscosity (Pa-s), shear stress (Pa), shear strain rate (1/s) and temperature (°C). Viscosity measurements were taken at intervals of 10 °C under thermal equilibrium conditions.

3.2.1. Calibration

The measured viscosity of PAO oil was compared to values given by the manufacturer. The difference between the measured and the given viscosities is within 2.5% at 40 °C, 3.4% at 125 °C and 4.5% at low temperature of −18 °C as shown in Fig. 3. The error in the viscosity provided by the manufacturer is about ±3%, thus the measured viscosities are considered accurate.

3.2.2. Viscosity measurements results and analysis

The PAO/hNB nanofluids could exhibit Newtonian or non-Newtonian behavior depending on the concentration of NB, hence this needs to be verified. For this purpose, the viscosity versus strain rate curve for φ of 1% is shown by Fig. 4a for temperatures from −20 °C to 10 °C and by Fig. 4b from 20 °C to 70 °C. The viscosity does not change with shear strain rate (almost horizontal lines), which means the nanofluid is Newtonian. Similar behavior was observed for nanofluids with φ of 0.25% and 0.6%.

Another way to insure the Newtonian behavior of the nanofluid is the stress-strain relation as a function of temperature. The linear shear stress (τ) versus shear rate (ẏ) relation (Fig. 5), of the nanofluid with 1% concentration for the full temperature range including at −20 °C, confirms that the nanofluid is Newtonian. Results for 0.25% and 0.6% concentrations showed similar stress-strain trends confirming the Newtonian behavior as well.

The particle concentration effect on the viscosity is displayed in Fig. 6a as a function of temperature. As for typical Newtonian fluids, the viscosity increases with particle concentrations and decreases with increase in temperature.

3.2.3. Viscosity correlation

To develop a correlation for the PAO/hBN nanofluids, the viscosity-temperature relation is plotted in Fig. 6b as a function of volumetric concentration of the nano BN (0% is for the pure PAO).'Based on the rheological characteristics of the nanofluid shown in Figs. 5 and 6 above and using statistical analyses, a best fit model is reached using the LABFIT® software as follows:

$$\mu_{nf} = A\, e^{(BT+C\varnothing^2)} \tag{13}$$

where μ_{nf} is the viscosity of the nanofluid in Pa.s and T is in Kelvin units. Parameters A, B and C are characteristics of the nanofluid, each for certain temperature range and are provided in Table 1. In Eq. (13), nano particle concentration (φ) varies from 0 (for pure

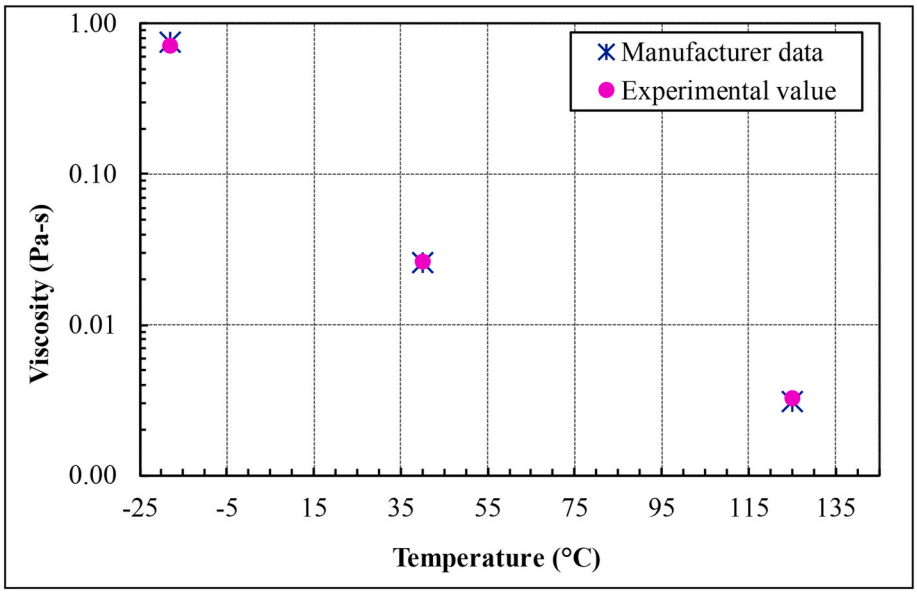

Fig. 3. Experimental viscosities of PAO vs manufacturer data.

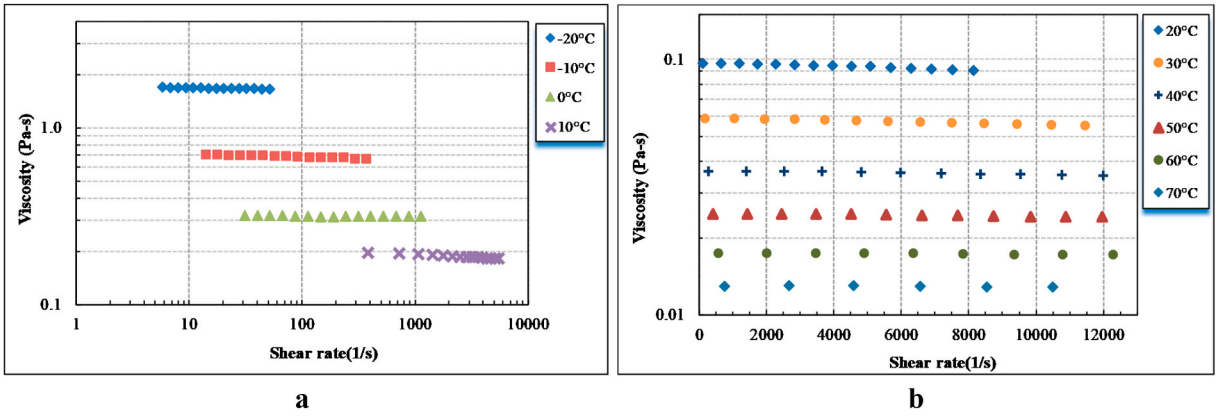

Fig. 4. Viscosity vs shear starin rate of PAO/hNB nanofluid of 1% φ for (a) −20 °C–10 °C and (b) 20 °C–70 °C.

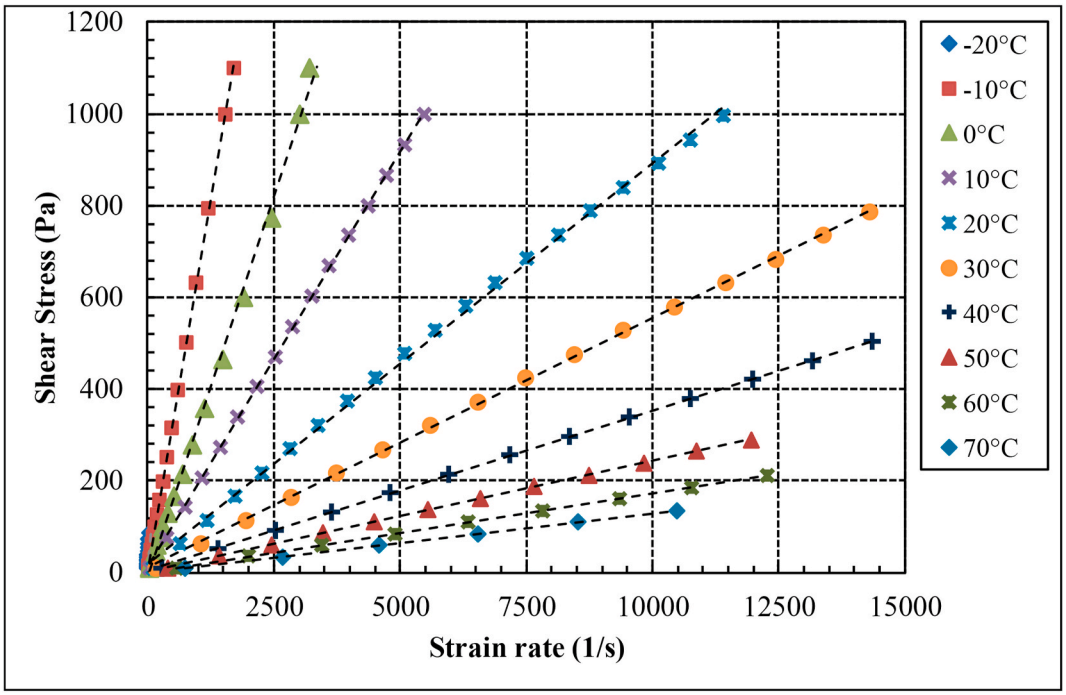

Fig. 5. Linear stress-strain relation for Newtonian PAO/hNB nanofluid of 1% φ

PAO) to 1. Eq. (13) predicts the viscosity values to within ±7% of the excremental values with $R^2 > 0.99$ for the full temperature range.

The developed correlation in Eq. (13) was compared to correlations available in open literature (cited in Ref. [19,42,51–54]) for predicting the viscosity of PAO/hBN nanofluids. Results of comparison showed that correlations in open literature gave a difference between 35% and 58% compared to Eq. (13) correlation predictions.

For subsequent Re and heat transfer calculations in present study, the viscosity of the nanofluids for different φ and temperatures were found from Eq. (13) correlation.

3.3. *Thermophysical properties for PAO/hBN nanofluids*

To evaluate the convective heat transfer of the nanofluids, in addition to the viscosity discussed in the previous section, values of the other thermophysical properties as a function of temperature and φ are needed. These are: the specific heat (Cp), density (ρ) and thermal conductivity (k) or thermal diffusivity (α).

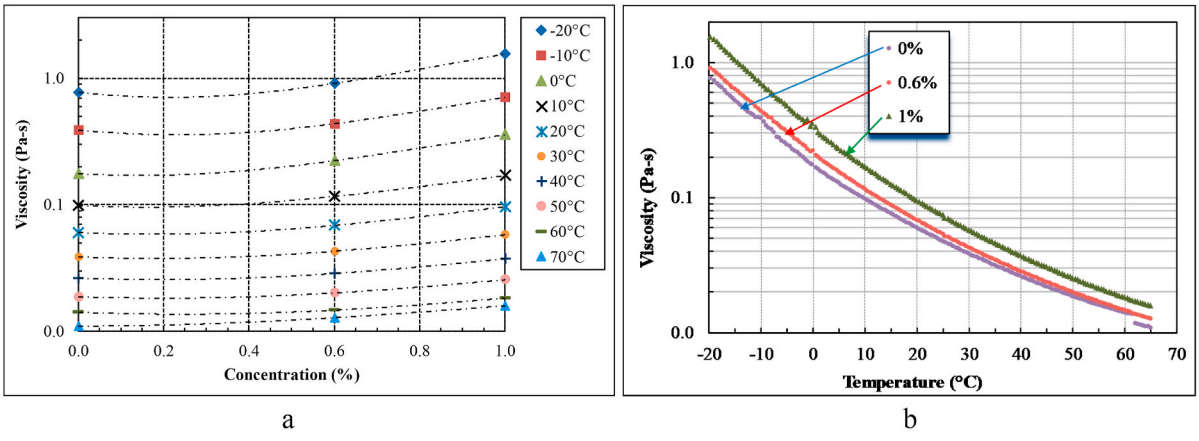

Fig. 6. (a) Viscosity vs (a) nanoparticle φ as a function of temperature, (b) temperature as a function of φ

Table 1
Parameters for Eq. 13

Parameters	Temperature range (253–273K)	Temperature range (273–293K)	Temperature range (293–313K)	Temperature range (313–383K)
A	0.29731×10^9	0.23611×10^7	0.39083×10^5	0.10167×10^4
B	−0.07813	−0.06011	−0.04568	−0.03379
C	0.71548×10^4	0.59373×10^4	0.43959×10^4	0.33323×10^4
R^2	0.99625	0.99447	0.99391	0.99245

3.3.1. *Specific heat of PAO/hBN nanofluid*

Differential Scanning Calorimetry (DSC) is used to measure the specific heat of the nanofluids and pure PAO as a function of temperature. Results are shown in Fig. 7a. The results show that the specific heat for PAO increases with the temperature by about 44% from 45 °C to 95 °C. However, the specific heat for the nanofluid with $\varphi = 1\%$ was found to be enhanced by about 48% at high temperatures compared to pure PAO. This increase in Cp of nanofluids can be attributed to several factors including: (1) the size and the shape of the NB nanoparticles changes the phonon spectrum from continuous to discrete, which leads to increasing *Cp*. (2) due to changes in atom vibrations as a results of adding the solid BN nanoparticles. (3) the higher *Cp* of the BN nanoparticle may have resulted in additional energy storage.

3.3.2. *Thermal diffusivity and thermal conductivity*

Laser flash apparatus is used to measure the thermal diffusivity as a function of the temperature for the nanofluid and pure PAO. The results are shown by Fig. 7b. While the pure PAO thermal diffusivity decreases slightly with temperature (Fig. 7b), a rapid increase in thermal diffusivity with temperature was observed for the nanofluid. Based on the measured thermal diffusivity of the nanofluid, the thermal conductivity of the nanofluid can be calculated from Eq. (14) and is shown in Fig. 7c:

$$\alpha = k / \rho\, Cp \tag{14}$$

The thermal conductivity (k) of nanofluids increases significantly compared to pure PAO and it increases by increasing φ up to 1%. k is decreasing with temperature for both pure PAO and the nanofluids unlike other nanofluids investigated in open literature for which the base fluid k decreases with temperature, while its nanofluid k increases with temperature.

3.4. *Heat transfer experimental results*

Heat transfer experiments were conducted for Re range from 3000 to 18,000 by controlling the mass flow rate of the fluids and the heat input of the electric heater. A series of experiments of forced convective heat transfer for 0.25, 0.6 and 1 vol% PAO/hBN nanofluids was carried out with local nanofluid temperature for heat transfer performance calculations of 36–70 °C. The temperature difference between the inner test section wall and the fluid, a key parameter in minimizing experimental errors, was above 12 °C in all cases. Nusselt number is calculated as a function of Re using the procedure outlined in section 2 above and using the measured properties reported in this section above. The experimental uncertainty for the convective heat transfer coefficient (calculated according to the procedures detailed in [57] and [58]) was within 4% for all experiments. Fig. 8 shows Nu versus Re for PAO and for the nanofluids. Nu for PAO was compared to results obtained using the correlation that was given in Eqs. (11) and (12) and also shown in

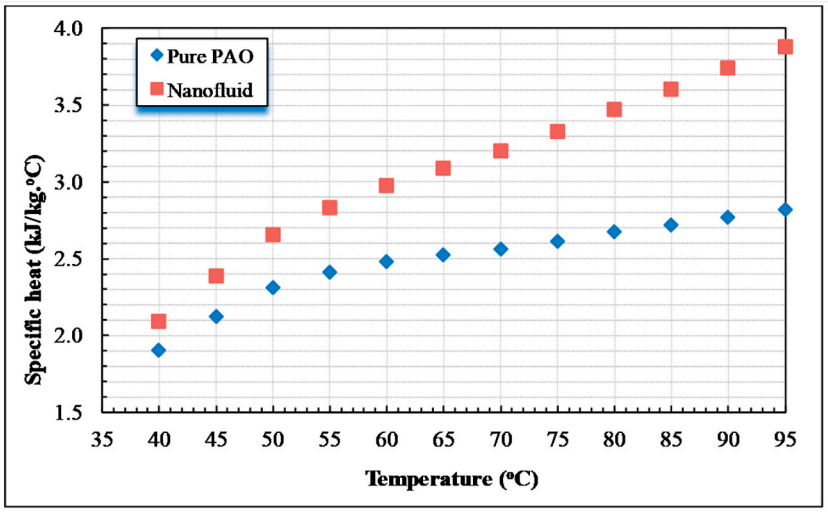

(a)

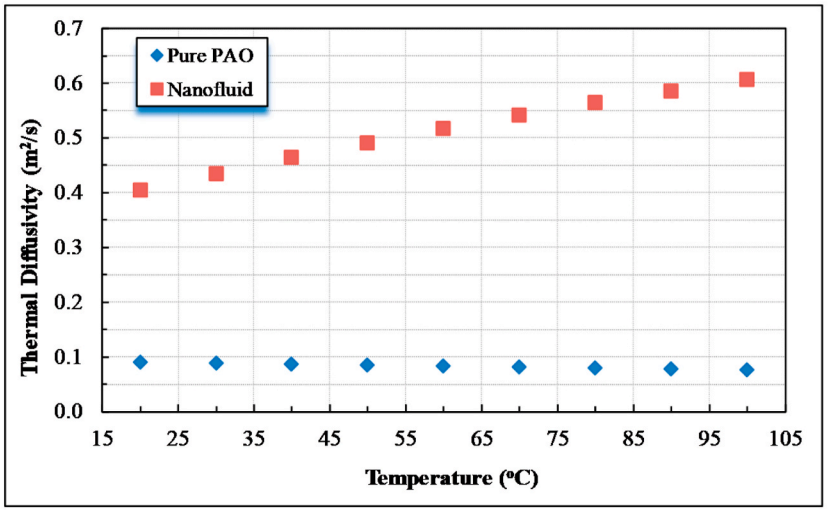

(b)

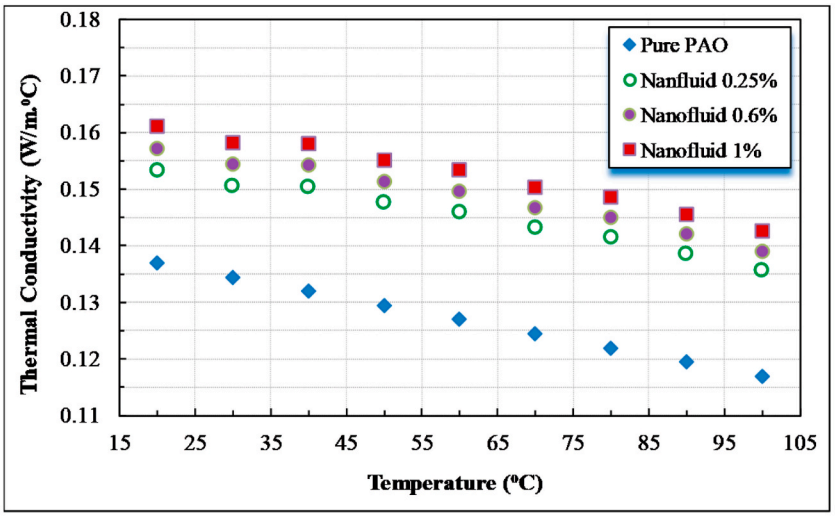

(c)

(caption on next page)

Fig. 7. (a) Specific heat, (b) Thermal diffusivity and (c) Thermal conductivity vs temperature for PAO/hNB nanofluid of 1% volumetric concentration.

Fig. 8. The correlation results under predicted Nu by a maximum amount of 9% compared to the measured values of pure PAO oil. Nu enhancement is shown in Fig. 9 for PAO/hBN nanolfuids with different concentrations and is compared to Nu of pure PAO. This enhancement is expressed in terms of the ratio of nanofluid Nu to PAO oil. Nu is enhanced by an average and maximum of 10%–13%, 17%–20% and 26%–29% for NB φ of 0.25%, 0.6% and 1%, respectively.

The viscosity of the PAO/hBN nanofluids is larger than the PAO base fluid, so the experiments were run at higher velocities for the nanofluids to reach the same Re as for the PAO. An alternative approach was used in Ref. [13] by having constant velocity for the base fluid and the nanofluid experimental runs and then comparing their heat transfer performance, which resulted in lower heat transfer coefficient, h for the Al2O3/water nanofluid that they used compared to the water base fluid. A fair and more reasonable comparison would be the one with the same Re as in the present study despite the increase in the required pumping power. The increase in Nu for the pure PAO shown in Fig. 8 is attributed mainly to enhancement in h (at the same k) as Re increases (U increases at the same ρ, D and μ). The increase in Nu with Re for the PAO/hBN nanofluids (Fig. 8) for all φ cases is attributed to the increase in h as Re increases compared to h of the base fluid. The increase in h is more than the increase in k of the nanofluids, which resulted in Nu increase ($Nu = h\,D/k$). There are two competing phenomena that affect h of nanofluids. When k increases, the resistance to thermal diffusion in the laminar sublayer of the boundary layer decreases, which would increase h. At the same time, the higher viscosity of the nanofluids causes the thickness of the sublayer to increase, hence its resistance to heat transfer. These two competing and conflicting phenomena cause the increase/decrease (depending on the class of nanofluids) in h. For the PAO/hBN nanofluids investigated in the present work, it is clear that the first phenomena (increase in k) has won over the second phenomena (increase in μ) resulting in Nu increase.

The potential of the PAO/hBN nanofluids developed in the present study can be evaluated using the Mouromtseff number Mo [46, 55] for turbulent flow. Mo is defined as a function of all thermophysical properties of the nanofluids that are also included in Gnielinski correlation [49,50]:

$$Mo = \frac{k^{0.8}\,\rho^{0.67}\,Cp^{0.33}}{\mu^{0.47}} \tag{15}$$

Using Eq. (15), the Mo of the base fluid and the nanofluid can be compared under constant velocity condition and the fluid with better heat transfer is the one with higher Mo. The ratio of the Mo for PAO/hBN to that of PAO base fluid in this study is found equal to 0.93. As a comparison, this ratio was found in Ref. [56] equal to o.75 for Al2O3/water nanofluid and 0.89 for the SiC/water nanofluid.

4. Conclusions

The heat transfer performance of a new class of nanofluids of Boron Nitrite nanoparticles dispersed in PAO oil base fluid is investigated experimentally. The thermophysical properties (viscosity, specific heat, thermal diffusivity and conductivity) of the nanofluid are measured and appropriate relations are derived as a function of temperature and nano particle concentration. An experimental setup is designed and built to measure the heat transfer coefficient of both base fluid and nanofluid as a function of

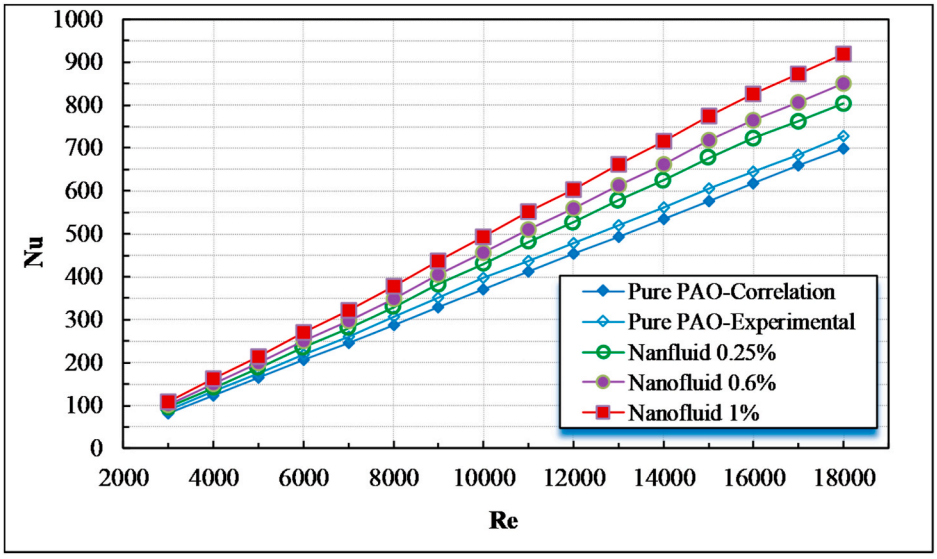

Fig. 8. Nusselt number VS Reynolds number for PAO/hNB nanofluida and for PAO.

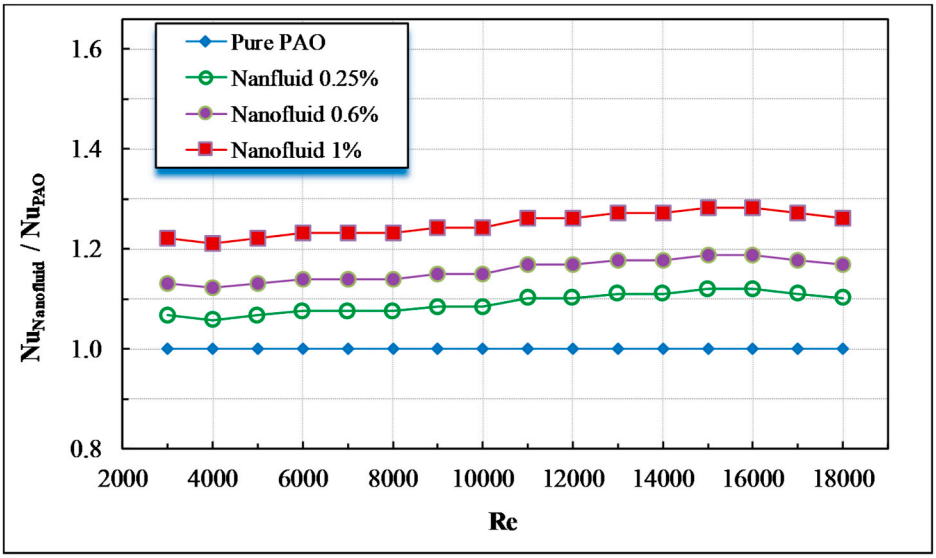

Fig. 9. Nusselt number enhancement VS Reynolds number for PAO/hNB nanofluids compared to PAO.

Reynolds number. The following findings and conclusions are made:

- The developed PAO/hNB nanofluids exhibit Newtonian behavior as a function of temperature (from −20 to 70 °C) and BN volume concentration φ (0.25–1%).
- The viscosity decreases with temperature for both PAO and PAO/hNB nanofluids and increases with φ.
- A viscosity correlation based on experimental data is developed that predicts the viscosity of PAO/hNB nanofluids as a function of temperature and φ to within 7% of the experimental values.
- The specific heat increases with temperature by 44% from 45 °C to 95 °C for PAO and by 48% for the nanofluid with $\varphi = 1\%$.
- The thermal conductivity (k) of nanofluids increases significantly compared to pure PAO and it increases by increasing φ up to 1%. k is decreasing with temperature for both pure PAO and the nanofluids unlike other nanofluids in open literature.
- The heat transfer enhancement in terms of Nussel Number (Nu) presented as the ratio of nanofluid Nu to PAO oil, showed average and maximum values of 10%–13%, 17%–20% and 26%–29% for NB φ of 0.25%, 0.6% and 1%, respectively.
- Two competing phenomena affect the heat transfer performance of nanofluids: the increase/decrease in resistance to thermal diffusion in the laminar sublayer when k increases and viscosity decreases, respectively. For the PAO/hBN nanofluids in the present work, the first phenomena (increase in k) caused the heat transfer enhancement.

Author statement

All persons who meet authorship criteria are listed as authors, and all authors certify that they have participated sufficiently in the work, including participation in the concept, design, analysis, writing, or revision of the manuscript.

Declaration of competing interest

The authors declare that they have no known competing financial interests or personal relationships that could have appeared to influence the work reported in this paper.

Acknowledgments

This publication was supported by the International Research Collaboration Co Fund Grant [IRCC-2019-012], Qatar University, Qatar. The findings achieved herein are solely the responsibility of the authors.

References

[1] L. Yang, et al., A review of heating/cooling processes using nanomaterials suspended in refrigerants and lubricants, Int. J. Heat Mass Tran. 153 (2020) 119611, https://doi.org/10.1016/j.ijheatmasstransfer.2020.119611.
[2] N.A. Che Sidik, M. Mahmud Jamil, W.M.A. Aziz Japar, I. Muhammad Adamu, A review on preparation methods, stability and applications of hybrid nanofluids, Renew. Sustain. Energy Rev. (2017), https://doi.org/10.1016/j.rser.2017.05.221.
[3] K. Khanafer, K. Vafai, A review on the applications of nanofluids in solar energy field, Renew. Energy (2018), https://doi.org/10.1016/j.renene.2018.01.097.
[4] D. Wen, G. Lin, S. Vafaei, K. Zhang, Review of nanofluids for heat transfer applications, Particuology (2009), https://doi.org/10.1016/j.partic.2009.01.007.

[5] D.K. Devendiran, V.A. Amirtham, A review on preparation, characterization, properties and applications of nanofluids, Renew. Sustain. Energy Rev. (2016), https://doi.org/10.1016/j.rser.2016.01.055.

[6] R. Saidur, K.Y. Leong, H.A. Mohammed, A review on applications and challenges of nanofluids, Renew. Sustain. Energy Rev. (2011), https://doi.org/10.1016/j.rser.2010.11.035.

[7] M. Ghalandari, A. Maleki, A. Haghighi, M. Safdari Shadloo, M. Alhuyi Nazari, I. Tlili, Applications of nanofluids containing carbon nanotubes in solar energy systems: a review, J. Mol. Liq. (2020), https://doi.org/10.1016/j.molliq.2020.113476.

[8] M. Krishnam, S. Bose, C. Das, Boron nitride (BN) nanofluids as cooling agent in thermal management system (TMS), Appl. Therm. Eng. 106 (2016) 951–958, https://doi.org/10.1016/j.applthermaleng.2016.06.099.

[9] A.K. Sleiti, Rheological characteristics of boron nitride nanofluids with polyalpha-olein oil base fluid, in: ASME International Mechanical Engineering Congress and Exposition IMECE, 2011.

[10] A.K. Sleiti, J.S. Kapat, An experimental investigation of liquid jet impingement and single-phase spray cooling using polyalphaolefin, Exp. Heat Tran. 19 (2) (2006), https://doi.org/10.1080/08916150500479349.

[11] M.H. Ahmadi, A. Mirlohi, M. Alhuyi Nazari, R. Ghasempour, A review of thermal conductivity of various nanofluids, J. Mol. Liq. (2018), https://doi.org/10.1016/j.molliq.2018.05.124.

[12] H. Hong, D. Thomas, A. Waynick, W. Yu, P. Smith, W. Roy, Carbon nanotube grease with enhanced thermal and electrical conductivities, J. Nanoparticle Res. 12 (2) (2010) 529–535, https://doi.org/10.1007/s11051-009-9803-y.

[13] W. Yu, D.M. France, D.S. Smith, D. Singh, E.V. Timofeeva, J.L. Routbort, Heat transfer to a silicon carbide/water nanofluid, Int. J. Heat Mass Tran. 52 (15–16) (2009) 3606–3612, https://doi.org/10.1016/j.ijheatmasstransfer.2009.02.036.

[14] D. Singh, et al., An investigation of silicon carbide-water nanofluid for heat transfer applications, J. Appl. Phys. (2009), https://doi.org/10.1063/1.3082094.

[15] M.S. Liu, M. Ching-Cheng Lin, I. Te Huang, C.C. Wang, Enhancement of thermal conductivity with carbon nanotube for nanofluids, Int. Commun. Heat Mass Tran. 32 (9) (2005) 1202–1210, https://doi.org/10.1016/j.icheatmasstransfer.2005.05.005.

[16] S.U.S. Choi, Z.G. Zhang, W. Yu, F.E. Lockwood, E.A. Grulke, Anomalous thermal conductivity enhancement in nanotube suspensions, Appl. Phys. Lett. (2001), https://doi.org/10.1063/1.1408272.

[17] J.A.N. Bazan, Thermal Conductivity of Poly-Alpha-Olefin (PAO)-based Nanofluids, M.S. Thesis, *Univ. Dayt.*, 2010.

[18] B. Ilhan, M. Kurt, H. Ertürk, Experimental investigation of heat transfer enhancement and viscosity change of hBN nanofluids, Exp. Therm. Fluid Sci. 77 (2016) 272–283, https://doi.org/10.1016/j.expthermflusci.2016.04.024.

[19] M. Ramezanizadeh, M.A. Nazari, Modeling thermal conductivity of Ag/water nanofluid by applying a mathematical correlation and artificial neural network, Int. J. Low Carbon Technol. 14 (4) (2019) 468–474, https://doi.org/10.1093/ijlct/ctz030.

[20] A. Komeilibirjandi, A.H. Raffiee, A. Maleki, M. Alhuyi Nazari, M. Safdari Shadloo, Thermal conductivity prediction of nanofluids containing CuO nanoparticles by using correlation and artificial neural network, J. Therm. Anal. Calorim. 139 (4) (2020) 2679–2689, https://doi.org/10.1007/s10973-019-08838-w.

[21] M. Ramezanizadeh, M. Alhuyi Nazari, M.H. Ahmadi, G. Lorenzini, I. Pop, A review on the applications of intelligence methods in predicting thermal conductivity of nanofluids, J. Therm. Anal. Calorim. 138 (1) (2019) 827–843, https://doi.org/10.1007/s10973-019-08154-3.

[22] E.V. Timofeeva, W. Yu, D.M. France, D. Singh, J.L. Routbort, Nanofluids for heat transfer: an engineering approach, Nanoscale Res. Lett. (2011), https://doi.org/10.1186/1556-276X-6-182.

[23] M. Fares, M. AL-Mayyahi, M. AL-Saad, Heat transfer analysis of a shell and tube heat exchanger operated with graphene nanofluids, Case Stud. Therm. Eng. 18 (2020) 100584, https://doi.org/10.1016/j.csite.2020.100584. October 2019.

[24] A. Siricharoenpanich, S. Wiriyasart, A. Srichat, P. Naphon, Thermal cooling system with Ag/Fe3O4 nanofluids mixture as coolant for electronic devices cooling, Case Stud. Therm. Eng. 20 (2020) 100641, https://doi.org/10.1016/j.csite.2020.100641. April.

[25] A.H.A. Al-Waeli, K. Sopian, H.A. Kazem, M.T. Chaichan, Evaluation of the electrical performance of a photovoltaic thermal system using nano-enhanced paraffin and nanofluids, Case Stud. Therm. Eng. 21 (2020) 100678, https://doi.org/10.1016/j.csite.2020.100678. October 2019.

[26] S. Wiriyasart, C. Hommalee, S. Sirikasemsuk, R. Prurapark, P. Naphon, Thermal management system with nanofluids for electric vehicle battery cooling modules, Case Stud. Therm. Eng. 18 (2020) 100583, https://doi.org/10.1016/j.csite.2020.100583. December 2019.

[27] A.H. Alami, A.A. Hawili, K. Aokal, M. Faraj, M. Tawalbeh, "Enhanced heat transfer in agitated vessels by alternating magnetic field stirring of aqueous Fe–Cu nanofluid, Case Stud. Therm. Eng. 20 (2020) 100640, https://doi.org/10.1016/j.csite.2020.100640. December 2019.

[28] S. Hashimoto, K. Kurazono, T. Yamauchi, Anomalous enhancement of convective heat transfer with dispersed SiO2 particles in ethylene glycol/water nanofluid, Int. J. Heat Mass Tran. 150 (2020), https://doi.org/10.1016/j.ijheatmasstransfer.2019.119302.

[29] V. Sridhara, L.N. Satapathy, Effect of nanoparticles on thermal properties enhancement in different oils-A review, Crit. Rev. Solid State Mater. Sci. 40 (6) (2015) 399–424, https://doi.org/10.1080/10408436.2015.1068159.

[30] A. Refiei, R. Loni, G. Najafi, A.Z. Sahin, E. Bellos, Effect of use of MWCNT/oil nanofluid on the performance of solar organic Rankine cycle, Energy Rep. 6 (2020) 782–794, https://doi.org/10.1016/j.egyr.2020.03.035.

[31] T.S.Y. Moh, T.W. Ting, A.H.Y. Lau, Graphene Nanoparticles (GNP) nanofluids as key cooling media on a flat solar panel through micro-sized channels, Energy Rep. 6 (2020) 282–286, https://doi.org/10.1016/j.egyr.2019.11.075.

[32] K. Ali, A. Ahmed, S. Hussain, I. Khan, I. Tlili, Enhancement of heat transfer rate of solar energy via rotating Jeffrey nanofluids using Caputo – fabrizio fractional operator: an application to solar energy, Energy Rep. 5 (2019) 41–49, https://doi.org/10.1016/j.egyr.2018.09.009.

[33] Z. Huang, et al., Electrical and thermal properties of insulating oil-based nanofluids: a comprehensive overview, IET Nanodielectrics 2 (1) (2019) 27–40, https://doi.org/10.1049/iet-nde.2018.0019.

[34] M. Gulzar, et al., Tribological performance of nanoparticles as lubricating oil additives, J. Nanoparticle Res. 18 (8) (2016) 1–25, https://doi.org/10.1007/s11051-016-3537-4.

[35] Y. Wang, et al., Comparative evaluation of the lubricating properties of vegetable-oil-based nanofluids between frictional test and grinding experiment, J. Manuf. Process. 26 (2017) 94–104, https://doi.org/10.1016/j.jmapro.2017.02.001.

[36] E.D. Ramón-Raygoza, C.I. Rivera-Solorio, E. Giménez-Torres, D. Maldonado-Cortés, E. Cardenas-Alemán, R. Cué-Sampedro, Development of nanolubricant based on impregnated multilayer graphene for automotive applications: analysis of tribological properties, Powder Technol. 302 (2016) 363–371, https://doi.org/10.1016/j.powtec.2016.08.072.

[37] Q. Wan, Y. Jin, P. Sun, Y. Ding, Tribological behaviour of a lubricant oil containing boron nitride nanoparticles, Procedia Eng. 102 (2015) 1038–1045, https://doi.org/10.1016/j.proeng.2015.01.226.

[38] M.J.G. Guimarey, M.J.P. Comuñas, E.R. López, A. Amigo, J. Fernández, Thermophysical properties of polyalphaolefin oil modified with nanoadditives, J. Chem. Thermodyn. 131 (2019) 192–205, https://doi.org/10.1016/j.jct.2018.10.035.

[39] S.S.K. Kiu, S. Yusup, C.V. Soon, T. Arpin, S. Samion, R.N.M. Kamil, Tribological investigation of graphene as lubricant additive in vegetable oil, J. Phys. Sci. 28 (2017) 257–267, https://doi.org/10.21315/jps2017.28.s1.17.

[40] I.M. Mahbubul, R. Saidur, M.A. Amalina, Latest developments on the viscosity of nanofluids, Int. J. Heat Mass Tran. (2012), https://doi.org/10.1016/j.ijheatmasstransfer.2011.10.021.

[41] L.S. Sundar, K.V. Sharma, M.T. Naik, M.K. Singh, Empirical and theoretical correlations on viscosity of nanofluids: a review, Renew. Sustain. Energy Rev. (2013), https://doi.org/10.1016/j.rser.2013.04.003.

[42] J.P. Meyer, S.A. Adio, M. Sharifpur, P.N. Nwosu, The viscosity of nanofluids: a review of the theoretical, empirical, and numerical models, Heat Tran. Eng. (2016), https://doi.org/10.1080/01457632.2015.1057447.

[43] L. Syam Sundar, E. Venkata Ramana, M.K. Singh, A.C.M. Sousa, Thermal conductivity and viscosity of stabilized ethylene glycol and water mixture Al2O3 nanofluids for heat transfer applications: an experimental study, Int. Commun. Heat Mass Tran. (2014), https://doi.org/10.1016/j.icheatmasstransfer.2014.06.009.

[44] S. Aberoumand, A. Jafarimoghaddam, M. Moravej, H. Aberoumand, K. Javaherdeh, Experimental study on the rheological behavior of silver-heat transfer oil nanofluid and suggesting two empirical based correlations for thermal conductivity and viscosity of oil based nanofluids, Appl. Therm. Eng. (2016), https://doi.org/10.1016/j.applthermaleng.2016.01.148.
[45] A.A. Minea, Hybrid nanofluids based on Al2O3, TiO2 and SiO2: numerical evaluation of different approaches, Int. J. Heat Mass Tran. (2017), https://doi.org/10.1016/j.ijheatmasstransfer.2016.09.012.
[46] I.C. Nelson, D. Banerjee, R. Ponnappan, Flow loop experiments using polyalphaolefin nanofluids, J. Thermophys. Heat Tran. 23 (4) (2009) 752–761, https://doi.org/10.2514/1.31033.
[47] B.A.K. Naik, A.V. Vinod, Heat transfer enhancement using non-Newtonian nanofluids in a shell and helical coil heat exchanger, Exp. Therm. Fluid Sci. 90 (2018) 132–142, https://doi.org/10.1016/j.expthermflusci.2017.09.013. April 2017.
[48] H. Shahmohamadi, R. Rahmani, H. Rahnejat, C.P. Garner, N. Balodimos, Thermohydrodynamics of lubricant flow with carbon nanoparticles in tribological contacts, Tribol. Int. 113 (2017) 50–57, https://doi.org/10.1016/j.triboint.2016.12.048. December 2016.
[49] Incropera, DeWitt, Bergman, Lavine, Fundamental of Heat and Mass Transfer, sixth ed., 2007.
[50] V. Gnielinski, Neue Gleichungen für den Wärme- und den Stoffübergang in turbulent durchströmten Rohren und Kanälen, Forsch. Im. Ingenieurwes. 41 (1) (1975) 8–16, https://doi.org/10.1007/BF02559682.
[51] M. Hemmat Esfe, H. Rahimi Raki, M.R. Sarmasti Emami, M. Afrand, Viscosity and rheological properties of antifreeze based nanofluid containing hybrid nano-powders of MWCNTs and TiO2 under different temperature conditions, Powder Technol. (2019), https://doi.org/10.1016/j.powtec.2018.10.032.
[52] L. Yang, J. Xu, K. Du, X. Zhang, Recent developments on viscosity and thermal conductivity of nanofluids, Powder Technol. (2017), https://doi.org/10.1016/j.powtec.2017.04.061.
[53] S. Ghasemi, A. Karimipour, Experimental investigation of the effects of temperature and mass fraction on the dynamic viscosity of CuO-paraffin nanofluid, Appl. Therm. Eng. (2018), https://doi.org/10.1016/j.applthermaleng.2017.09.021.
[54] A. Karimipour, S. Ghasemi, M.H.K. Darvanjooghi, A. Abdollahi, A new correlation for estimating the thermal conductivity and dynamic viscosity of CuO/liquid paraffin nanofluid using neural network method, Int. Commun. Heat Mass Tran. (2018), https://doi.org/10.1016/j.icheatmasstransfer.2018.02.002.
[55] M. Rebay, Y. Kabar, S. Kakaç, Microscale and Nanoscale Heat Transfer: Analysis, Design, and Application, *CRC Press*, 2016, https://doi.org/10.1201/b19261-12.
[56] S.A. Putnam, D.G. Cahill, P.V. Braun, Z. Ge, R.G. Shimmin, Thermal conductivity of nanoparticle suspensions, J. Appl. Phys. 99 (8) (2006), https://doi.org/10.1063/1.2189933.
[57] Ahmad Sleiti, Mohammad Salehi, Stephen Idem, Detailed velocity profiles in close-coupled elbows—Measurements and computational fluid dynamics predictions (RP-1682), Science and Technology for the Built Environment 23 (8) (2017) 1212–1223, https://doi.org/10.1080/23744731.2017.1285176.
[58] Mohammed Shublaq, Ahmad Sleiti, Experimental Analysis of Water Evaporation Losses in Cooling Towers Using Filters, Applied Thermal Engineering 175 ((2020) 115418) (2020) 1–10, https://doi.org/10.1016/j.applthermaleng.2020.115418.